A model of indirect cell death caused by tumor vascular damage after high-dose radiotherapy

Abstract

Purpose: To present a radiobiological model of indirect tumor cell death caused by vascular damage in high-dose hypofractionated radiotherapy.

Methods and Materials: Tumor oxygenation is obtained by solving the reaction-diffusion equation, with a capillary network created according to a vascular fraction and distribution of capillary sizes. Tumor cells die according to the linear-quadratic model with oxygen enhacement ratios. Radiation also kills endothelial cells (ECs): if the death of ECs in any given capillary depletes a cross section of the capillary (functional sub-unit) the capillary becomes non-functional. Such capillary *death* will affect tumor oxygenation, driving tumor cells in the vicinity into severe hypoxia. Capillaries can recover function in time due to ECs proliferation. Tumor cells entering a pre-determined severe hypoxia status are tagged and killed according a hypoxia death model. We have compared our model with experimental results on indirect cell death.

Results: Our model can reproduce experimental results of indirect cell death with realistic parameters. The decrease in surviving fraction with time is due to EC and capillary death, which causes indirect cell killing. Our results show that capillary damage and indirect cell death are important for doses ≥15 Gy.

Conclusions: We present a dynamic model of indirect cell death caused by tumor vascular damage after high-dose radiotherapy, based on first principles and experimental data. The model can fit recently experimental data that shows the effect of *indirect* cell death in tumors grown in mice.

1. Introduction

Developments in radiotherapy treatment delivery have lead to a situation where high-dose fractions can be safely delivered [1]. This has boosted the use of Stereotactic Body Radiation Therapy (SBRT) and Stereotactic Radiation Surgery (SRS) [2-4].

There is an intense debate on the radiobiology of large radiation doses [5-10]. There are studies that suggest that, in addition to direct cell death, high-doses may cause *indirect* cell death. Such effect seems to be two-fold: i) high-doses may trigger an immune-response against the tumor [9,11,12], and; ii) may produce vascular damage, causing cell starvation and death [7,9,13]. A seminal experimental study showed that damage of capillaries triggered tumor cell death and increased control [14]. A critical analysis by Brown *et al* showed that control obtained with SBRT can be explained by dose escalation, with no need for *new biology* [8]. Park *et al* reviewed many clinical and pre-clinical experimental results, finding evidence of vascular damage at high-doses [15]. A recent experimental report showed that high single fraction doses (15-30 Gy) caused *indirect* cell death in pre-clinical models [13]. On the other hand, another study claim that endothelial cell death does not play a significant role in tumor control after investigating a genetically modified tumor mouse model with hyper-radiation-sensitive endothelial cells [16]. It seems that vascular damage happen at large doses, but its role in tumor control is still debatable.

Despite the increasing experimental literature on *indirect* tumor cell death caused by vascular damage, efforts on modelling this effect have been limited. Recently, researchers at DKFZ have developed an analytical model of capillary death based on the inactivation of functional subunits (FSU) [17,18]. Paul-Gilloteaux *et al* have developed an in-silico tumor response model that includes endothelial cell damage and its effect in radiotherapy response [19]. In this work we present a dynamical model of indirect tumor cell death triggered by damage of the tumor vascular system. The model is developed from first principles and experimental data, and includes: i) oxygenation of tumors according to the reaction-diffusion equation, ii) direct tumor cell death (linear-quadratic model), and re-oxygenation caused by this effect; iii) endothelial cell death, which can induce capillary death, and endothelial cell proliferation and recovery of capillary function; iv) tumor hypoxification due to vascular damage; v) indirect tumor cell death due to severe hypoxia; vi) evaluation of tumor control probability.

2. Methods and Materials

2.1. Sketch of the model

The flowchart of the model is presented in Figure 1. The pre-irradiation oxygenation of the tumor is calculated by solving the reaction-diffusion equation, with a capillary network created according to a certain vascular fraction and capillary radii. This oxygen distribution is pre-evaluated: regions with extreme hypoxia are treated like a pre-existing necrotic core, where cells are dead, local consumption is adjusted accordingly, and the oxygen distribution is recalculated. Then, oxygenation-dependent α and β values are calculated by including oxygen enhacement ratios (*OERs*). The tumor is irradiated, and tumor cells die according to the linear-quadratic (LQ) model. Radiation also kills endothelial cells (ECs) forming the vasculature of the tumor. If the death of ECs in any given capillary fulfills some predetermined conditions according to a capillary-death model, the capillary becomes non-functional and stops oxygenating the tumor, which we will refer to as capillary *death*. This will affect tumor oxygenation, driving tumor cells in the vicinity of non-functional capillaries into severe hypoxia. This effect competes with reoxygenation caused by tumor cell death. Capillaries can recover function in time due to ECs proliferation. Tumor cells entering a pre-determined severe hypoxia status are tagged and killed according a hypoxia-death model.

Rather than instantaneous cell death, we assume a progressive death to kinetic distributions. Finally, *direct*, *indirect* and overall surviving fractions are evaluated, and used to compute tumor control probabilities.

For the sake of computational simplicity, we assume that vascular fraction are homogeneous within the tumor (thus we can simulate only one voxel of the tumor). We also study only single-fraction treatments. More detailed information about the model is provided in the Supplementary Materials.

2.2. Oxygen distribution in the tumor and FEM solver.

The stationary state of the reaction-diffusion equation for oxygen distribution in a tumor voxel is [20,21]:

$$D\Delta u(\mathbf{x},t)=g(u(\mathbf{x},t)) \quad (1)$$

In the above equation $u(\mathbf{x},t)$ is the distribution of the oxygen, D its diffusion coefficient, and g is the oxygen consumption rate, which has the following form [22]:

$$g(u(\mathbf{x},t))=g_{max}\, u(\mathbf{x},t)/(u(\mathbf{x},t)+k) \quad (2)$$

We solve this equation in two spatial dimensions, which was shown to be a good surrogate of the 3D problem [22]. We have implemented a Matlab-based finite-element-method (FEM) solver [23]. Blood capillaries are assumed to be cylindrical, with a heterogeneous distribution of radii. There are experimental studies showing lognormal and exponential distributions of radii of tumor capillaries [24-26], and we have implemente both options in our model. Minimum and maximum radii limits are also imposed according to experimental studies. Blood capillaries are randomly positioned in a voxel according to a vascular fraction, *vf*, defined as the ratio of capillary area to total area [22]. The overlap of capillaries is explicitely avoided when generating the geometry. A steady 40 mmHg oxygen partial pressure is associated to capillaries by imposing Dirichlet conditions on their boundaries. Neumann conditions are applied to the flux of u at the outer boundary of the voxel. If the function of a capillary is destroyed by radiation at any time, that capillary is removed from the set of Dirichlet boundary conditions and it does not behave as an oxygen source anymore. The geometry is finely meshed, typically >10000 nodes for a 1 mm × 1 mm pixel.

2.3. Tumor cell death, kinetics and re-oxygenation.

Radiation induced cell tumor death is modelled with the LQ model,

$$log(SF_D^{\infty})=-\alpha(u)d-\beta(u)d^2 \quad (3)$$

where SF_D^{∞} is the surviving fraction, d the radiation dose, and α and β depend on the oxygenation of the cells as [27]:

$$\alpha(u)=\frac{\alpha_{ox}}{OER\alpha_m}\left(\frac{uOER\alpha_m+K_m}{u+K_m}\right) \quad (4)$$

$$\beta(u)=\frac{\beta_{ox}}{(OER\beta_m)^2}\left(\frac{uOER\beta_m+K_m}{u+K_m}\right)^2 \quad (5)$$

α_{ox}, β_{ox}, $OER\alpha_m$ and $OER\beta_m$ are the α-β values and the maximum enhancement ratios under fully aerobic conditions. K_m controls the slope of the curve.

We consider a progressive death of tumor cells that have been lethally damaged by radiation, *i.e.* cells do not die instantly but follow a given kinetic model. In this work we have used an exponential kinetic model to describe this effect as in [28], with half-life $t_{1/2}^{d} = log(2)/\lambda$. The fraction of death cells, which do not consume oxygen, is taken into account at each step by decreasing oxygen consumption accordingly in Equation (1).

2.4. EC and capillaries death.

We have implemented a model of capillary death based on the death of endothelial cells (EC) and the definition of functional subunits (FSUs). ECs conforming blood capillaries are assumed to die following the LQ model (OERs are not considered as these cells are well oxygenated):

$$log(SF_e^{\infty}) = -\alpha_e d - \beta_e d^2 \quad (6)$$

We consider that damaged ECs do not die instantly after irradiation, but follow a given kinetic curve. According to some experimental results [29-31] we have modelled such kinetics as a linear decrease with time,

$$SF_e(t) = \begin{cases} 1 - (1 - SF_e^{\infty} t)/t_e & \text{if } t < t_e \\ SF_e^{\infty} & \text{if } t \geq t_e \end{cases} \quad (7)$$

In this equation $SF_e(t)$ shows the evolution of the relative number of surviving ECs with time. The above equation is used to generate distributions to evaluate the probability of each EC of dying at each time step during the simulation.

Capillaries are assumed to have cylindrical geometry with length L and radius R. For simplicity we assume that all capillaries have the same length, but radii vary according to a probability distribution. ECs of size $dx*dy$ form the capillary wall. Thus, each capillary can be represented as a matrix with size dependent on L, R, dx and dy. A matrix describing the state of each EC (1=alive, 0=death) is created at the beginning of the simulation. After irradiation, each EC is randomly tagged as *lethaly damaged* or *undamaged*, according to Eq. (6). Cells tagged as *lethaly damaged* are then monitored during the simulation, and at each time step they are killed according to a probability distribution constructed from Eq. (7).

Capillary FSUs are defined as cross sections with n cells thickness. A capillary is killed if (and when) any FSU conforming it has been depleted (notice the overlap of different FSUs; capillary of length m cells will have $m-n+1$ FSUs of length n). This model is similar to that presented in [17], which used instead square-shaped FSUs to model capillary death.

Lost capillary function can be restored due to EC proliferation, which be assume will start after t_d. We assume that surviving ECs proliferate exponentially as $N_{EC}(t) = N_{EC,0}\, exp(\gamma t)$, where $N_{EC,0}$ is the number of ECs that are alive in the voxel after the delivery of the dose (therefore dose dependent). Newly generated cells take spots in the EC state matrix, and the function of capillaries is restored if those new cells calcel out the capillary death condition. No new capillaries are created due to EC proliferation, only recovery of already existing capillaries is allowed.

2.5. Indirect tumor cell death due to severe hypoxia

A model of indirect tumor cell death due to severe hypoxia has been developed based on experimental results [32,33]. We consider that cells below a certain oxygen threshold (u_{th}) can die due to the effect of severe hypoxia. The probability of death depends on the time that the cells stay in severe hypoxia. This relationship is well described by an exponential law [33]:

$$log(SF_H^{\infty})=-\mu t_h \tag{8}$$

In the above equation SF_H^{∞} represents the surviving fraction of a population of cells exposed to severe hypoxia during a time t_h ($t_{1/2}^H = log(2)/\mu$). Again, we use the symbol ∞ to denote that this surviving fraction is evaluated when all lethally damaged cells have died. Cells exposed to severe hypoxia do not die instantly. In fact, experimental results show that cells continue to die even after normal oxygenation has been re-established [32]. We have used a simple linear kinetic model to account for the death of cells that are (or have been) exposed to severe hypoxia:

$$SF_H(t')=\begin{cases} 1-(1-SF_H^{\infty}\, t')/t_H^{\infty} & \text{if } t' < t_H^{\infty} \\ SF_H^{\infty} & \text{if } t' \geq t_H^{\infty} \end{cases} \tag{9}$$

Time t' in the above equation is measured from the instant when cells enter in severe hypoxia. t_H^{∞} is the time at which we consider that every lethally damaged cell has died. Nodes entering/leaving severe hypoxia are tagged at each step of the calculation, and cells are killed according to the model above. There is one particularity with the implementation that is worth noticing here: as there is no way to know a priori how long cells will stay in severe hypoxia, the value of t_h (and SF_H^{∞}) in Eq. (8) is re-evaluated at each step of the simulation; this slightly changes the shape of the death kinetic model, but the effect is not important.

Direct and indirect cell death of tumor cells due to severe hypoxia will affect oxygen consumption and reoxigenation, as discussed in Section 2.2. Oxygen consumption is thus scaled as:

$$g_{rel}(\mathbf{x},t)=g_{max}\, SF_D(\mathbf{x},t)\, SF_H(\mathbf{x},t) \tag{10}$$

2.6. Most relevant experimental parameters.

Table I shows the most relevant parameters of the model. There are conflicting experimental reports on the radiosensitivity of ECs: in-vitro clonogenic assays point out a high radiosensitivity (α_e ~0.18 Gy) [34], but in-vivo experimental analyses show highly radio-resistant cells (α_e ~0.007 Gy) [29,30,35]. We have investigated different radiosensitivities of ECs. Li *et al* [30] observed progressive death of ECs after a large single dose of radiation until 16h post-irradiation, while Peña *et al* [29] observed a peak of apoptosis of ECs 12h post-irradiation, and much lower values of apoptosis 24h post-irradiation. Therefore, a value of t_e=16h seems appropiate.

Different lognormal and exponential distributions of capillary radii have been obtained from several publications [23-25]. We have investigated variable values of n to model capillary death. Regarding the doubling time t_d for EC proliferation, values in the range 2-10 days have been reported [15].

There is not much experimental evidence on the value of u_{th}. Some studies claim that below 1 mmHg cells can enter cell cycle arrest and eventually die [36,37]. On the other hand, Ljungkvist *et*

al [33] observed hypoxia turnover for cells with oxygen levels below 10 mmHg (cells marked with pimonidazole and CCI103F). We have not used such high thresholds, as they would results in a large percentage of cells affected by indirect death for standard vascular fractions even without the effect of capillary cell death.Values of $t_{1/2}^{H}$ have been mainly obtained from [32,33]. The latter study reported values ≈15h-50h, while the former observed progressive cell death 24h after cells had returned to normoxic status, therefore the term t_H^{∞} in our model to account for such effect. We have used $t_H^{\infty} \approx 2\text{-}3t_{1/2}^{H}$.

We have considered oxygen-dependent radiosensitivities for tumor cells [27], and $t_{1/2}^{D}$=120h [28].

2.7. Fit to Song's experimental data

In [13] tumors grown in mice were irradiated with single-doses (10-30 Gy), and surviving fractions evaluated at different times post-irradiation. They observed a marked decrease of the surviving fraction with time, which they attributed to *indirect* tumor cell death caused by vascular damage. Further analyses showed reduced blood perfusion and increased hypoxia in the tumor microenvironment. We have extracted SFs at different times post-irradiation (figure 1 in that paper) and used our model to fit the data. We also extracted data of Hoechst 33342 and pimonidazole uptake (figure 3) pre-irradiation and 48h after 20 Gy irradiation.

In order to fit experimental data, surviving fractions at each time t in our model were obtained by considering both dead and lethally damaged cells at that time (we assume that lethally damaged cells will not proliferate when planted). Therefore, this will include all cells killed or lethally damaged by radiation, which is delivered at time $t=0$, and cells killed or lethally damaged by severe hypoxia after irradiation. On the other hand, we have considered percentage of areas positive for Hoechst as a surrogate of capillary function, and pimonidazole uptake to shown living cells with u<10 mmHg [33].

We simulated a tumor with a homogeneous 4% vascular fraction and a lognormal distribution of capillary radii with maximum a minimum values of 2.8 and 26.7 μm, taken from [24]. We set $n=2$, t_e=16h, t_d= 72h, and $dx=dy$=10 μm in our capillary death model. We set a threshold oxygen pressure u_{th}=2 mmHg. We varyed α_{ox} and β_{ox}, α_e (α_e/β_e is set to 10 Gy) and $t_{1/2}^{H}$ for hypoxia cell death to obtain a good fit to the experimental results.

Results and Discussion

Fit of SFs at $t=0$ to the LQ model showed α and β values 0.13 Gy^{-1} and 0.0024 Gy^{-2} respectively. As those values are for tumors with heterogeneous oxigenation, and the input parameters of our model are α_{ox} and β_{ox}, fitted values were scaled up to account for hypoxia radio-resistance. Figure 2 shows the fit of our model to experimental data, with parameters α_{ox}=0.16 Gy^{-1}, β_{ox}=0.0028 Gy^{-2}, α_e=0.067 Gy^{-1}, and $t_{1/2}^{H}$=15h (mean and standard deviations of five simulations). Our model can qualitatively reproduce the experimental results. The decrease in surviving fraction with time is due to EC and capillary death, which causes severe hypoxia in the tumor. Our results show a steady decrease in time of SF for $d\geq$15 Gy. Experimental results showed for some doses a slight increase of SF between 3 and 5 days (not significant), which could be caused by accelerated proliferation, but that effect is not included in our model.

Surviving fractions of ECs with this parameters are 0.26, 0.08, 0.018, and 0.0003 for 10, 15, 20, and 30 Gy respectively, which results in severe damage to the capillary network for doses above 15 Gy, as shown in Figure 3. There is moderate vascular damage even for 10 Gy, but it does not result in

important indirect cell death because the remaining capillaries can maintain adequate oxygenation. Capillary funcionality is seriously damaged for doses above 15 Gy, but due to EC proliferation it can be recovered, but for 30 Gy where EC depletion is so harsh that proliferation cannot recover functionaly (within 5 days).

Percentage of functional capillaries 48h after irradiation with 20Gy is (5±2)%, not far from the ratio of Hoechst positive areas of (8±3)% extracted from [13]. On the other hand, the percentage of living cells with $u<10$ mmHg increases from (15±4)% before irradiation to (27±2)% 48h after irradiation, while pimonidazole positive area increases from (17±7)% to (21±3.5)% in [13].

In Figure 4 we show a qualitative representation of the spatio-temporal evolution of oxygenation, and surviving fractions associated to direct (dose) and indirect death (severe hypoxia) for an irradiation with 15 Gy. At $t=0$ the voxel has a heterogeneous distribution of oxigenation, including a necrotic core where $u<u_{th}$. 24h after irradiation most capillaries are non-functional, and many regions are in severe hypoxic conditions. Cells in dose regions are already dying, creating a heterogeneous map of indirect cell death (lower surviving fractions around non-functional capillaries). On the other hand, the map of direct cell death also presents heterogeneities, due to heterogeneities in oxygenation at the time of irradiation. 96h after irradiation many damaged capillaries have recovered function due to EC proliferation. That, and the death of many cells, leads to a fairly well oxygenated voxel. On the other hand, heterogeneities in direct, and specially indirect, cell death are more noticeable.

Conclusions

Indirect tumor cell death caused by vascular damage seems to play a role in high-dose hypofractionated radiotherapy. Modelling of this effect has not been extensively addresed in the literature despite the importance it might have for hypofractionated schedules. We present a dynamic model of direct and indirect cell death (caused by tumor vascular damage) after high-dose radiotherapy, based on first principles and experimental data. The model can fit recent experimental data that shows the effect of indirect cell death in tumors grown in mice.

Some effects have not yet been included in this model, for example cell diffusion and tumor shrinkage, or proliferation. We have assumed a homogeneous vascular fraction in order to simplify and speed up simulations: real tumors will have heterogeneous vascular fractions, which could be included in the model by averaging results for different simulations. Future refinements of the model will focus on extending the *biology* in the model, and implementing a 3D solver (even if radii of capillaries are sampled from realistic distributions, and 2D solutions seem to be a good representation of the 3D problem, they may miss some effects caused by the chaotic network of tumor capillaries).

This study constitutes a stepping stone towards modelling indirect tumor cell death caused by vascular damage.

References

1. Schlegel WC, Bortfeld T, Grosu AC (Editors). New Technologies in Radiation Oncology. New York: Springer Publishing Co; 2006.

2. Sperduto PW. A review of stereotactic radiosurgery in the management of brain metastases. Technol Cancer Res Treat 2003;2:105-110.

3. Chang BK, Timmerman RD. Stereotactic body radiation therapy: a comprehensive review. Am J Clin Oncol. 2007;30:637-644.

4. Lo SS, Fakiris AJ, Chang EL, et al. Stereotactic body radiation therapy: a novel treatment modality. Nat Rev Clin Oncol. 2010;7:44-54.

5. Kirkpatrick JP, Meyer JJ, Marks LB. The linear-quadratic model is inappropiate to model high dose per fraction effects in radiosurgery. Semin Radiat Oncol 2008:18;240-243.

6. Brenner DJ. The linear-quadratic model is an appropriate methodology for determining isoeffective doses at large doses per fraction. Semin Radiat Oncol 2008:18;234-239.

7. Song CW, Park H, Griffin RJ, Levitt SH. Radiobiology of Stereotactic Radiosurgery and Stereotactic Body Radiation Therapy. In: Lewitt SH, et al. Technical basis of Radiation Therapy: Practical Clinical Application. New York: Springer Publishing Co; 2012. p. 51-61.

8. Brown JM, Carlson DJ, Brenner DJ. The tumor radiobiology of SRS and SBRT: are more than the 5 Rs involved?. Int J Radiat Oncol Biol Phys. 2014;88:254-262.

9. Sperduto PW, Song CW, Kirkpatrick JP, Glatstein E. A hypothesis: indirect cell death in the radiosurgery era. Int J Radiat Oncol Biol Phys 2015:91;11-13.

10. Song CW, Kim M, Cho LC, Dusenbery K, Sperduto PW. Radiobiological basis of SBRT and SRS. Int J Clin Oncol 2014:19;570-578

11. Lee Y, Auh SL, Wang Y, et al. Therapeutic effects of ablative radiation on local tumor require CD8+ T cells: changing strategies for cancer treatment. Blood;114:589-595.

12. Zhang A, Niedermann G. Abscopal effects with hypofractionated schedules extending into the effector phase of the tumor-specific T cell response. Int J Radiat Oncol Biol Phys. 2018 IN PRESS

13. Song CW, Lee YJ, Griffin RJ, et al. Indirect Tumor Cell Death After High-Dose Hypofractionated Irradiation: Implications for Stereotactic Body Radiation Therapy and Stereotactic Radiation Surgery. Int J Radiat Oncol Biol Phys. 2015;93:166-172.

14. García-Barros M, Paris F, Cordón-Cardo C, Lyden D, Rafii S, Haimovitz-Friedman A, Fuks Z, Kolesnick R. Tumor response to radiotherapy regulated by endothelial cell apoptosis. Science. 2003;300:1155-1159.

15. Park HJ, Griffin RJ, Hui S, Levitt SH, Song CW. Radiation-induced vascular damage in tumors: implications of vascular damage in ablative hypofractionated radiotherapy (SBRT and SRS). Radiat Res. 2012;177:311-27.

16. Moding EJ, Castle KD, Perez BA, et al. Tumor cells, but not endothelial cells, mediate eradication of primary sarcomas by stereotactic body radiation therapy. Sci Transl Med 2015;7:278ra34.

17. Merrem A. Modeling of damage to the vasculature of the cerebral cortex after microbeam radiation therapy. MSc Thesis. University of Heidelberg 2013

18. Merrem A, Bartzsch S, Laissue J, Oelfke U. Computational modelling of the cerebral cortical microvasculature: effect of x-ray microbeams versus broad beam irradiation. Phys Med Biol. 2017;62:3902-3922.

19. Paul-Gilloteaux P, Potiron V, Delpon G, Supiot S, Chiavassa S, Paris F, Costes SV. Optimizing radiotherapy protocols using computer automata to model tumour cell death as a function of oxygen diffusion processes. Sci Rep. 2017;7(1):2280.

20. Daşu A, Toma-Daşu I, Karlsson M. Theoretical simulation of tumour oxygenation and results from acute and chronic hypoxia. Phys Med Biol 48:2003;2829-2842.

21. Mönnich D, Troost EG, Kaanders JH, et al. Modelling and simulation of [18F]fluoromisonidazole dynamics based on histology-derived microvessel maps. Phys Med Biol 2011;56:2045-57.

22. Espinoza I, Peschke P, Karger CP. A model to simulate the oxygen distribution in hypoxic tumors for different vascular architectures. Med Phys 2013:40;081703

23. Díaz-Botana P. Modeling chronic/acute hypoxia in tumors by solving the reaction/diffusion equation. MSc Thesis. University of Santiago de Compostela 2016

24. Konerding MA, Malkusch W, Klapthor B, et al. Evidence for characteristic vascular patterns in solid tumours: quantitative studies using corrosion casts. Brit J Cancer 1999:80;724-732.

25. Konerding MA, Fait E, Gaumann A. 3D microvascular architecture of pre-cancerous lesions and invasive carcinomas of the colon. Brit J Cancer 2001:84;1354-1362.

26. Tufto I, Lyng H, Rofstad EK. Vascular density in human melanoma xenografts: relationship to angiogenesis, perfusion and necrosis. Cancer Lett 1998:123;159-165.

27. Wouters BG, Brown JM. Cells at intermediate oxygen levels can be more important than the "hypoxic fraction" in determining tumor response to fractionated radiotherapy. Radiat. Res. 1997:147;541-550

28. Gago-Arias A, Aguiar P, Espinoza I, Sánchez-Nieto B, Pardo-Montero J. Modelling radiation-induced cell death and tumour re-oxygenation: local versus global and instant versus delayed cell death. Phys Med Biol 2016:61;1204-1216

29. Peña LA, Z. Fuks Z, Kolesnick RN. Radiation-induced apoptosis of endothelial cells in the murine central nervous system: protection by fibroblast growth factor and sphingomyelinase deficiency. Can Res 2000:60;321-327.

30. Li YQ, Chen P, Haimovitz-Friedman A, Reilly RM, Wong CS. Endothelial apoptosis initiates acute blood brain disruption after ionizing radiation. Can Res 2003:63;5950-5956.

31. Donker M, Van Furth WR, Mulder-Van Der Kracht S, et al. Negligible radiation protection of endothelial cells by vascular endothelial growth factor. Oncol Rep. 2007;18:709-714.

32. Steinbach JP, Wolburg H, Klump A, Probst H, Weller M. Hypoxia-induced cell death in human malignant glioma cells: energy deprivation promotes decoupling of mitochondrial cytochrome c release from caspase processing and necrotic cell death. Cell Death Differ 2003:10;823-832.

33. Ljungkvist AS, Bussink J, Kaanders JH, et al. Hypoxic cell turnover in different solid tumor lines. Int J Radiat Oncol Biol Phys 2005:62;1157-1168.

34. Riquier H, Wera AC, Heuskin AC, Feron O, Lucas S, Michiels C. Comparison of X-ray and alpha particle effects on a human cancer and endothelial cells: survival curves and gene expression profiles. Radiother Oncol. 2013;106:397-403.

35. Lyubimova NV, Coultas PG, Yuen K, Martin RF. In vivo radioprotection of mouse brain endothelial cells by Hoechst 33342. Br J Radiol 2001;74:77-82.

36. Harriss-Phillips WM, Bezak E, Yeoh E. The HYP-RT hypoxic tumour radiotherapy algorithm and accelerated repopulation dose per fraction study. Comput Math Methods Med. 2012;2012:363564.

37. Ljungkvist ASE, Bussink J, Rijken PF, et al. Vascular architecture, hypoxia, and proliferation in first generation xenografts of human head-and-neck squamous cell carcinomas. Int J Radiat Oncol Biol Phys 2002:54;215-228.

Figure Captions

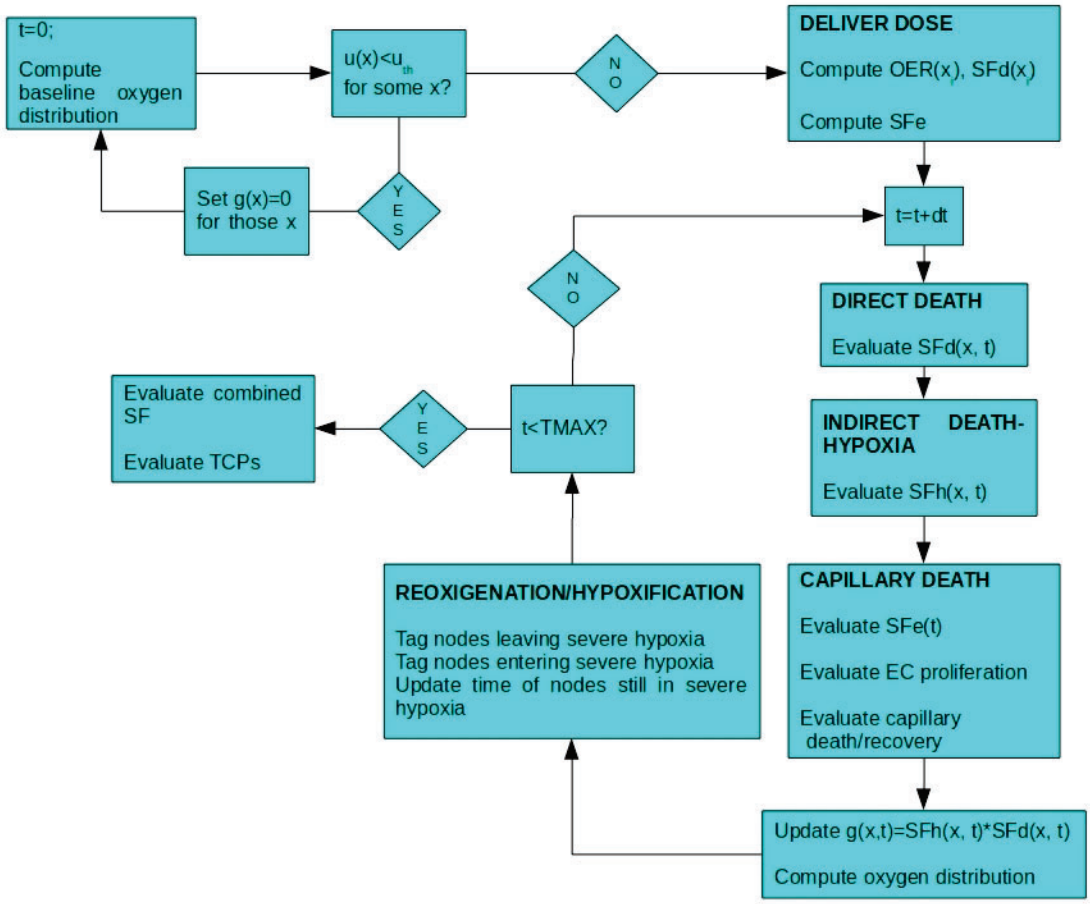

Figure 1: Sketch of the flowchart of the model.

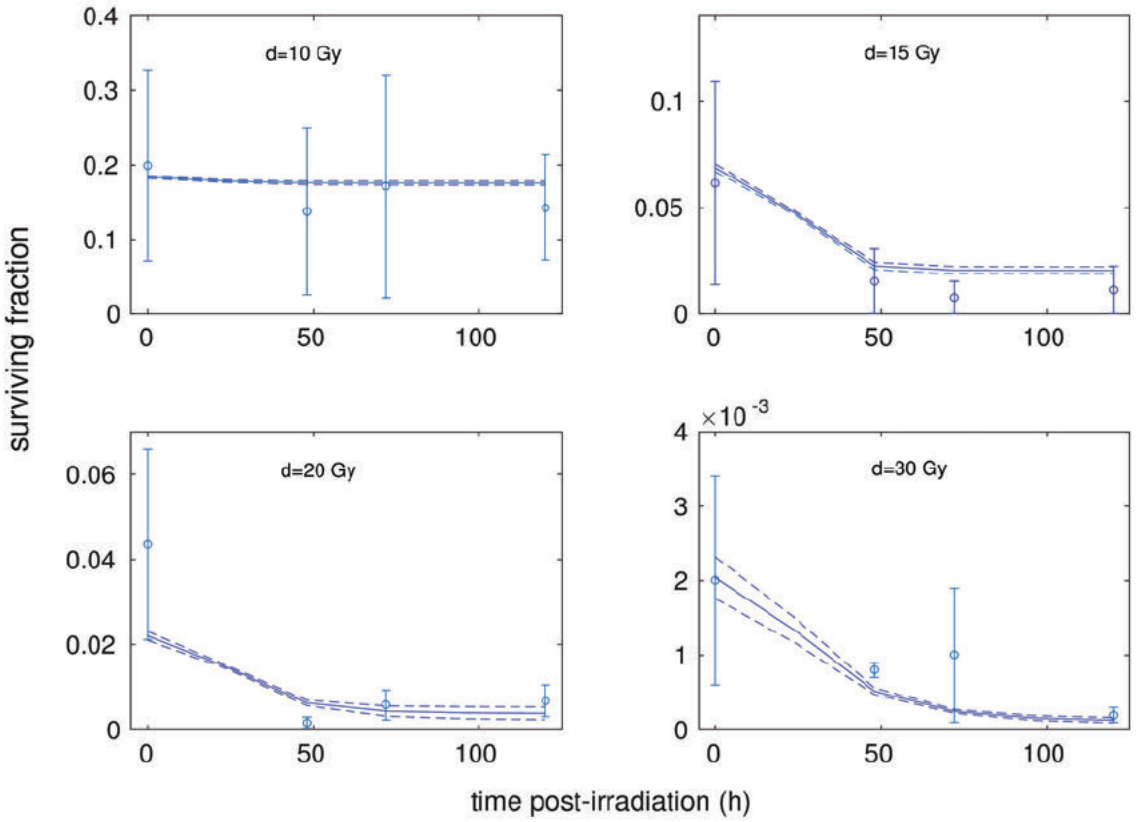

Figure 2: Surviving fractions at different times post-irradiation with different doses: experimental data taken from [13] (o) and model results: mean (solid lines) and ±1 standard deviation (dashed lines) of five simulations.

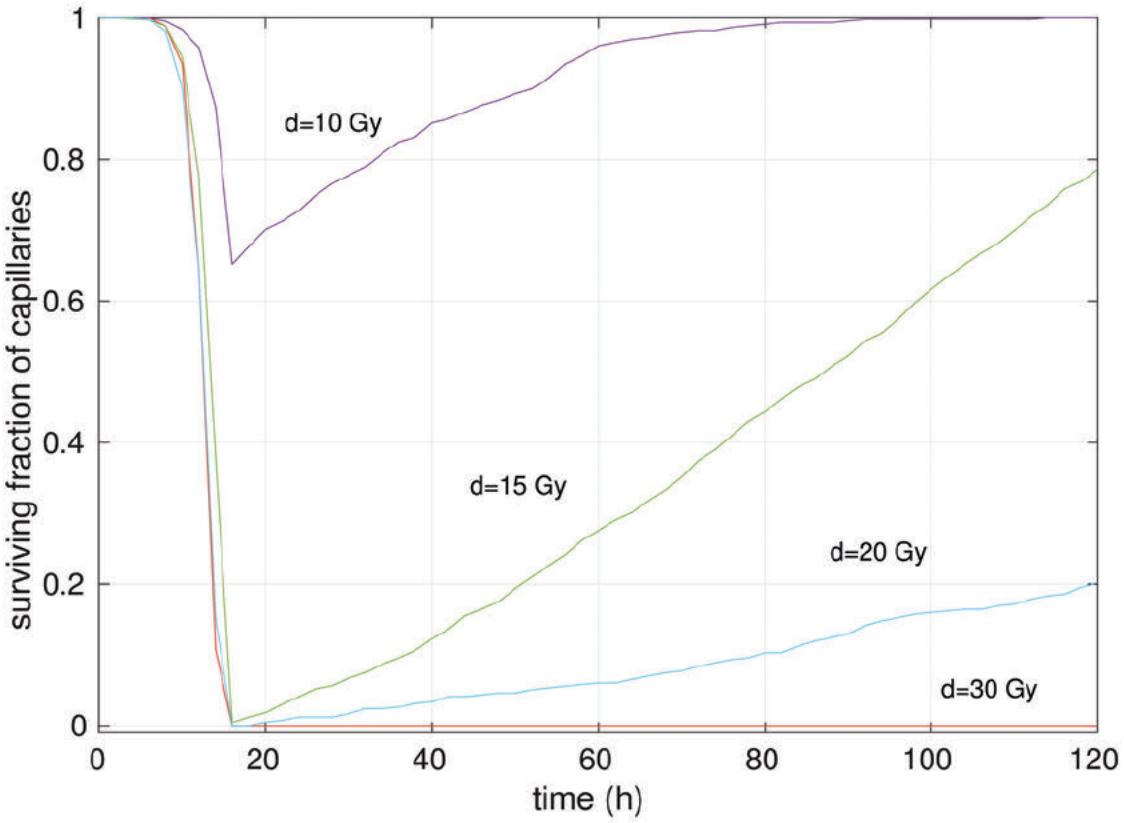

Figure 3: Functionality of capillaries versus time post-irradiation obtained with our model.

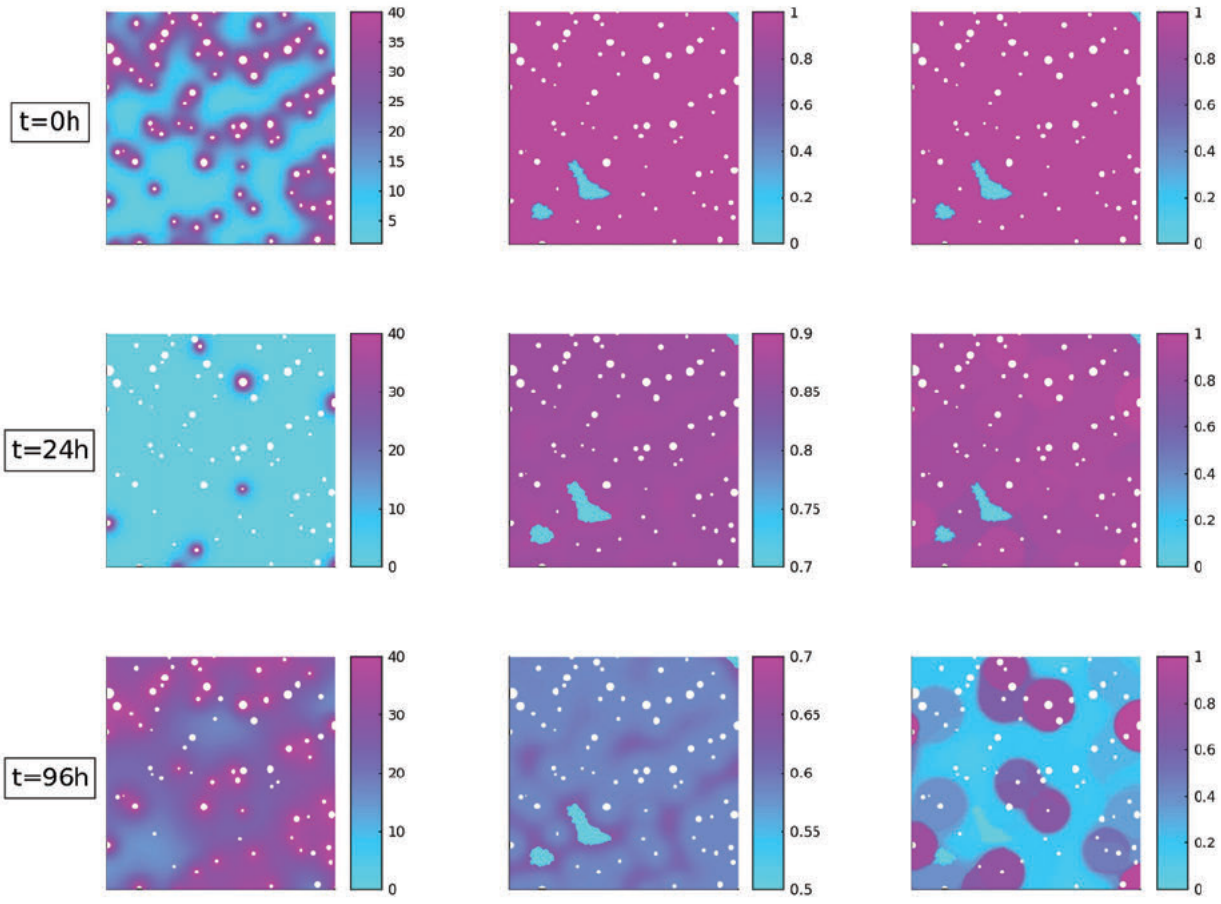

Figure 4. Qualitative representation of the spatio-temporal evolution of oxygenation (left), and surviving fractions associated to direct death (center) and indirect death (right). White circles are capillaries. Notice the different colormap scale in the central panels, in order to highlight the effect of OERs on the surviving fraction.